

RESEARCH

Open Access



CCT8 drives colorectal cancer progression via the RPL4-MDM2-p53 axis and immune modulation

Yangyang Teng^{1†}, Hao Lin^{1†}, Zijian Lin^{1†}, Xichen Li^{1†}, Yejiao Ruan¹, Binhui Pan², Jinlin Ge¹, Yuesheng Zhu¹, Daopo Lin¹, Qingji Ying¹, Zhenzhai Cai^{1*} and Xuanping Xia^{1*}

Abstract

Purpose Colorectal cancer (CRC) ranks high in global mortality, emphasizing the need for effective interventions. The aim of the research is to elucidate the oncogenic role of CCT8 in CRC and its interaction with RPL4 in the RPL4-MDM2-p53 axis.

Methods TIMER 2.0, TCGA, and GTEx databases were used to analyze CCT8 expression patterns in CRC. Immunohistochemistry was performed to examine CCT8 distribution in CRC tissues and adjacent non-tumor tissues. Functional assays, including CCK-8, transwell, wound-healing, and flow cytometry, were conducted using DLD-1 and HCT116 cell lines to assess the effects of CCT8 on cell proliferation, migration, invasion, and apoptosis. Gene set enrichment analysis, protein-protein interaction network analysis, and co-immunoprecipitation were performed to explore the interaction between CCT8 and RPL4 and their role in the RPL4-MDM2-p53 pathway. Additionally, gene set variation analysis was applied to investigate the relationship between CCT8/RPL4 expression and immune infiltration patterns in CRC.

Results CCT8 was significantly upregulated in CRC and associated with tumor progression. Mechanistically, CCT8 potentially synergizes with RPL4 concluded from their positive correlation and similar immune infiltration patterns, influencing the RPL4-MDM2-p53 axis and contributing to p53 ubiquitination and degradation.

Conclusion These findings underscore the oncogenic significance of CCT8 in CRC and shed light on its molecular mechanisms, paving the way for potential therapeutic applications.

Keywords CCT8, RPL4, Colorectal cancer, Immune infiltration, p53 signaling pathway

[†]Yangyang Teng, Hao Lin, Zijian Lin and Xichen Li contributed equally to this work.

*Correspondence:

Zhenzhai Cai
caizhenzhai@wmu.edu.cn
Xuanping Xia
feyxh@163.com

¹Department of Gastroenterology, Second Affiliated Hospital and Yuying Children's Hospital of Wenzhou Medical University, Wenzhou, China

²Department of Nephrology, Wenzhou Central Hospital, Wenzhou, China



Introduction

Cancer-related deaths stemming from colorectal cancer (CRC) rank as the third most common cause of mortality globally among individuals of all ages [1]. Over the past decade, the Global Cancer Statistics Survey reported a 6.1% incidence and a 9.2% mortality rate for CRC [2]. Recent advancements in colonoscopy technology have significantly reduced incidence and mortality rates [3]. However, a considerable number of patients diagnosed with early-stage CRC have already developed metastases, given the inconspicuous nature of their clinical symptoms. Furthermore, advanced CRC presents a grim prognosis and proves challenging to treat, thus constituting a major global health concern. The progression from epithelium or gland to CRC is widely acknowledged to be driven by multiple genes and factors [4]. Consequently, exploring new risk factors and understanding the pathogenic mechanisms of CRC is of utmost importance for the development of comprehensive strategies for prevention and treatment.

The cytoplasmic chaperonin-containing TCP1 complex (CCT), also known as the TCP1 ring complex, is a molecular chaperone essential for proper protein folding in eukaryotic cells [5, 6]. Among its subunits, CCT8 has recently emerged as a critical player in tumor biology, implicated in the promotion of CRC proliferation, invasion, and metastasis through the LASP1-WTp53 axis [7]. Thus, the correlation between CCT8 and p53 in CRC was worthy of further study. Functioning as a tumor suppressor, p53 activates downstream signaling pathways to inhibit abnormal division and initiate DNA repair. Additionally, p53 triggers apoptosis in the presence of irreversible DNA damage, thereby preventing cancer development [8, 9]. Recent studies highlight the significant role of p53 protein ubiquitination in the apoptosis signaling pathway, relying on the concerted participation of E1, E2 and E3 ubiquitin ligases. The murine double minute 2 (MDM2), one of the E3 ubiquitin-protein ligases, serves as the primary regulator of p53, promoting p53 degradation by forming a stable complex through the MDM2 and p53 N-terminal domains [10]. Ribosomal protein (RP) L4, integral components of ribosomes, has been identified as a potential modulator of the MDM2-p53 axis, though its precise role in CRC remains unclear [11]. Through bioinformatic analysis, we observed a significant upregulation of CCT8 in various cancers, especially in colorectal, gastric, and bile duct cancers. Experimental validation confirmed the significant upregulation of CCT8 expression in CRC tissues, particularly in tissues with higher malignancy. Further evidence demonstrated that CCT8 enhances MDM2-mediated p53 ubiquitination and degradation by interacting with RPL4. Immunological analysis also revealed that CCT8, as a

potential co-expressed gene with RPL4, exhibits a similar pattern of immune infiltration.

In summary, our study delves into the oncogenic mechanisms of CCT8 in CRC, particularly in regulating the behavior of tumor cells through the RPL4-MDM2-p53 pathway. The significance of this research lies in uncovering novel mechanisms of CCT8 in CRC, laying the foundation for personalized treatment and targeted interventions. We believe that these findings will open new possibilities for the treatment of CRC patients and provide robust support for further exploration in the field of tumor biology.

Materials and methods

Data acquisition

CCT8 expression data and related clinical information were retrieved from The Cancer Genome Atlas (TCGA) and Genotype-Tissue Expression (GTEx) databases via the UCSC Xena platform. Pan-cancer difference analysis of CCT8 expression across 17 types malignancies was performed using TIMER 2.0 (<https://cistrome.shinyapps.io/timer/>). Validation of expression in CRC was conducted using The Gene Expression Omnibus (GEO) datasets (<https://www.ncbi.nlm.nih.gov/geo/>, ID: GSE17536).

GSEA

As a computational method, Gene Set Enrichment Analysis (GSEA) is utilized to determine whether a predefined set of genes shows statistically significant agreement between two biological states (such as phenotype). To judge the contribution to the phenotype, the distribution trend of the group of genes in the gene table were ranked by the phenotype correlation according to the difference. GSEA was performed to analyze Kyoto Encyclopedia of Genes and Genomes (KEGG) pathways. Adjusted p values < 0.05 , enrichment of standardized scores ($|NES| < 1$, and false discovery rate (FDR) < 0.05 were considered significant differences.

GSVA

As a non-parametric and unsupervised method, Gene Set Variation Analysis (GSVA) is utilized to evaluate the enrichment of gene sets in relation to mRNA expression data. In this study, we used the single-sample GSEA method from the R package GSVA (version 3.6). Each gene set was comprehensively scored by the GSVA algorithm, and the potential differences in biological functions between the high- and low-risk groups were evaluated.

STRING

As a comprehensive database, STRING (<https://string-db.org/>) aims to collect, score, and integrate all publicly available sources of protein-protein interaction (PPI)

data and complement these with computational predictions of potential functions. R software was used for correlation analysis of CCT8, with an interaction score of 0.4 (p values < 0.01). We used STRING to develop and construct related proteins and PPI networks and analyze the interactions among related proteins, and we visualized them with the MCODE APP in CYTOSCAPE 3.7.2.

Cell lines and transfection

HEK293T and HCT116 cells were purchased from the Chinese Academy of Science Cell Bank (Shanghai, China). Cells were cultured in RPMI 1640 medium (Gibco, NY, USA) with 10% fetal bovine serum (Gibco, NY, USA) and incubated at 37 °C in a humidified atmosphere of 5% CO₂.

For transfection, HEK293T or HCT116 cells were seeded in 12-well plates (12 × 10⁴ cells per well). Transfection was performed using Lipofectamine 8000 reagent according to the manufacturer's instructions (Beyotime, Shanghai, China).

Cell viability assay

The Cell Counting Kit 8 (CCK-8, Dojindo, Japan) was utilized to determine the proliferation of CRC cells. Briefly, cells were trypsinized, resuspended in complete medium, and counted. Cells were seeded in 96-well plates at a density of 3000–5000 cells per well (adjusted based on cell growth rates) in 100 µL of medium per well. Each experimental group was set up in 3 replicates. After seeding, plates were then incubated in a cell culture incubator.

Starting from the second day after seeding, 10 µL of CCK-8 reagent was added to each well 2–4 h before the end of the culture period. After 4 h of incubation, the plates were placed on a shaker and gently agitated for 2–5 min. The optical density (OD) at 450 nm was measured using a microplate reader (Tecan infinite, Austria). Data were analyzed to evaluate cell proliferation.

Cell migration assay

Cells were trypsinized, resuspended in complete medium to form a cell suspension, and counted. Cells were seeded in 96-well plates at a density determined by cell size (typically 50,000 cells/well) to ensure 90% confluency the next day. Plates were incubated at 37 °C with 5% CO₂. The next day, the medium was replaced with low-serum medium. A scratch was made in the center of each well using a scratch tool. Each group was set up in triplicate, with a culture volume of 100 µL per well. Wells were gently washed 2–3 times with serum-free medium to remove detached cells. Low-serum medium was added, and images were taken at 0 h to record the initial scratch. Plates were incubated at 37 °C with 5% CO₂. At appropriate time points based on wound closure, plates were scanned using the Celigo instrument (Nexcelom, Beijing,

China). Migration area was analyzed using Celigo software to evaluate cell migration ability.

Cell apoptosis assay

A cell suspension was collected when the cells in the 6-well plates of each experimental group reach approximately 70%. Each group should be set up in triplicate (cell count $\geq 5 \times 10^5$ per treatment). Centrifuge at 1300 rpm for 5 min and wash the cell pellet with pre-cooled PBS at 4 °C. Wash the cell pellet once with 1 × binding buffer, centrifuge at 1300 rpm for 3 min, and collect the cells. Resuspend the cell pellet in 200 µL of 1 × binding buffer. Add 10 µL of Annexin V-APC staining solution and incubate at room temperature in the dark for 10–15 min. Depending on the cell count, add 400–800 µL of 1 × binding buffer and proceed to flow cytometry analysis (BD, American) and finally analyze the results. Apoptosis kit (eBioscience, Shanghai, China).

Cell invasion assay

Cell invasion assays were performed using a invasion kit (Corning, Shanghai, China). Briefly, the chambers were removed from the –20 °C freezer and placed into a new 24-well plate, followed by equilibration to room temperature under sterile conditions. To rehydrate the Matrigel matrix layer, 500 µL of serum-free medium was added to both the upper and lower chambers, and the plate was incubated at 37 °C for 2 h. A serum-free cell suspension was prepared, and the cell concentration was adjusted to 10⁵ cells per well (24-well plate) based on preliminary optimization. After rehydration, the chambers were transferred to a new plate, and the medium in the upper chamber was carefully removed and 200 µL of the cell suspension was added. The lower chamber was filled with 750 µL of medium containing 30% FBS. The plate was then incubated at 37 °C. Following incubation, the chambers were inverted onto absorbent paper to remove the medium. Non-invasive cells on the inner surface of the chambers were gently removed using a cotton swab. Migrated cells on the lower surface of the membrane were stained with 2–3 drops of staining solution for 3–5 min, rinsed several times, and air-dried. Images were captured using a microscope (OLYMPUS, Shanghai, China), with 4 random fields per chamber imaged at 100X magnification and 9 random fields at 200X magnification. The number of migrated cells per field was counted from the 200X images, and statistical analysis was performed to compare the invasive ability between experimental and control groups. Data are presented as the mean number of migratory cells per field ± standard deviation. A T-Test was used to determine statistical significance, with $p < 0.05$ considered statistically significant.

Cell cycle detection

Cell cycle analysis was performed using propidium iodide (PI) (Sigma, Shanghai, China) analysis. When cells in 6 cm dishes reached approximately 80% confluency (ensuring cells were not in the plateau phase), they were trypsinized, resuspended in complete medium, and collected into 5 mL centrifuge tubes. Each experimental group was prepared in triplicate, with a minimum of 10^6 cells per sample. The cell suspension was centrifuged at 1300 rpm for 5 min, and the supernatant was discarded. The cell pellet was washed once with ice-cold DPBS (pH 7.2–7.4) and centrifuged again at 1300 rpm for 5 min. The cell staining solution was prepared by mixing 40× PI stock solution (2 mg/mL), 100× RNase (Thermo Fisher Scientific, Shanghai, China) stock solution (10 mg/mL), 1× DPBS, and 25× Triton X-100 (Sigma, Shanghai, China) in a ratio of 25:10:1000:40, respectively. The cell pellet was resuspended in an appropriate volume of staining solution to achieve a flow rate of 300–800 cells per second during analysis. Samples were then analyzed using a flow cytometer (BD, American). Data analysis was performed using NovoExpress software to determine cell cycle distribution.

Co-immunoprecipitation (Co-IP)

Cells were harvested and lysed with RIPA buffer (Beyotime, Shanghai, China) in 10-cm dishes for 15 min. After centrifugation for 15 min at 14,000 g, the supernatant was collected after centrifugation and cocultured with Dynabeads protein A and IgG antibody or primary antibody at 4 °C overnight. Subsequently, the beads were washed 3 times with RIPA buffer. Finally, 60 μL of 2X loading buffer was added to the beads, and then the immunoprecipitates were boiled at 100 °C for 5 min.

Western blotting

Western blotting Cells were seeded in 6-well plates and lysed using RIPA buffer (Beyotime). BSA were used as common standard and the concentration of sample proteins were calculated. Then 5X loading buffer was added to the supernatant and boiled at 100 °C for 10 min. The SDS-PAGE gels were prepared for blotting onto PVDF membranes. TBST with 5% skim milk was used to block the membrane for 30 min. Then the PVDF membranes were cut according to the molecular size of each target protein from the instruction and ensured the target protein was within at least two locating markers before being incubated with primary antibody at 4 °C overnight. Subsequently, the PVDF membranes were incubated with horseradish peroxidase-conjugated secondary antibody for 2 h at 37°C. Finally, the target bands were detected with ECL reagent. The above experiments were repeated 3 times for each target protein to ensure

the reproducibility and reliability and the blots and gels were attached in Supplementary Files.

Glutathione-S-transferase (GST) pull-down assay

The recombinant plasmid was transformed into *E. coli* BL21 for GST-CCT8 fusion protein. According to the manufacturer's protocol, the fusion proteins were purified and immobilized with sepharose. Then, the purified GST-CCT8 fusion protein and GST control with sepharose were suspended and incubated with 20 μl His-RPL4 fusion protein at 4 °C for 8 h under gentle rotation. After elution and centrifugation, the bound proteins were separated by SDS-PAGE and analyzed by western blotting.

Immunohistochemistry

The paraffin embedded Sects. (3–5 mm) for each tissue were prepared appropriately. After deparaffinized and hydrated with xylene and ethanol, the sections were heated with sodium citrate antigen repair solution (Cell Signaling Technology, Boston, USA) and kept at subboiling temperature (95–98°C) for 10 min. Next, the cooled and cleaned sections were incubated with primary antibody at 4 °C overnight and then incubated with fluorescent-conjugated secondary antibody, which was repeated for another antibody. Axio Vert. A1, the inverted fluorescence microscope (ZEISS, Oberkochen, Germany) was utilized for section imaging.

Quantitative real-time PCR

TRIzol reagent (Invitrogen, Shanghai, China) was used to extract total RNA from cells. Reverse transcription was performed according to the manufacturer's direction. Amplification reactions were carried out by using amplification primers with SYBR Green PCR Master Mix (Sangon Biotech, Shanghai, China), and the reaction volumes were 20 μl containing 2 μl of cDNA for each set of experiments. Subsequently, ABI StepOne Plus was used for PCR analysis.

Statistical analysis

To ensure the accuracy and reliability of data analysis, we employed multiple statistical approaches. For samples from the TCGA database, assuming data independence and normal distribution, Student's t-test was used to compare the expression levels of the CCT8 gene between tumor tissues and paired normal tissues. For CRC immunohistochemical samples, One-way ANOVA was performed to analyze differences in CCT8 gene expression rates among tumor tissues with different degrees of differentiation, under the assumption of data independence and normal distribution, with error bars represented as standard deviation (SD). For categorical data, such as the pathological data of CRC immunohistochemical samples, the Chi-square test was used to compare differences in

CCT8 gene expression levels among patients with different clinicopathological parameters. Survival analysis was conducted using the Kaplan-Meier method, with grouping based on the median expression level of the CCT8 gene to compare survival time differences between groups. Considering interactions among different factors, Two-way ANOVA was performed to assess the effects of CCT8 knockdown on p53 expression at different time points under ActD treatment conditions, with error bars represented as standard error of the mean (SEM). The correlation between genes or between genes and signaling pathways was evaluated using the Spearman rank correlation coefficient. For CCK-8 assay data, considering interactions between different treatment groups (e.g., ShCon and ShCCT8) and different time points, Two-way ANOVA was applied, with error bars also represented as SEM. In addition, One-way ANOVA was used to compare differences in apoptosis and proliferation rates among different treatment groups, with error bars represented as SD. Statistical significance levels were set as $P < 0.05$, $P < 0.01$, and $*P < 0.001$.

Results

CCT8 expression is upregulated in CRC tissue

To conduct a preliminary assessment of the role of CCT8 in cancer, we utilized the Timer 2.0 Network server (<http://timer.comp-genomics.org/>) to analyze the mRNA expression levels of CCT8 across various types of cancer. As depicted in Fig. 1A, CCT8 expression was significantly elevated in 17 cancers, including CRC, gastric cancer, and bile duct cancer. Furthermore, we conducted additional verification which revealed a significant upregulation of CCT8 expression compared to adjacent normal tissue (Fig. 1B, C). Immunohistochemical analysis further confirmed the differential expression of CCT8 in CRC (Fig. 1D). Adjacent normal tissues exhibited low levels of CCT8 expression, while poorly differentiated CRC tissues displayed significantly higher levels of CCT8 compared to well-differentiated tissues (Figs. 1E-G). These findings suggest that CCT8 may function as an oncogene and contribute to CRC development. Moreover, the expression level of CCT8 was significantly correlated with histological grade, metastasis status, TNM stage, and mean survival time in CRC patients. However, no correlation was observed between CCT8 expression and patient age, sex, tumor location, or tumor size (survival analysis was performed using the Kaplan-Meier method, and Chi-square test to examine the association between CCT8 expression and clinicopathological parameters) (Table 1).

CCT8 promotes CRC cell proliferation, migration, and invasion in vitro

To further clarify the effect of CCT8 on CRC cells, we performed experiments using DLD-1 and HCT116 cell lines. Real-time qPCR was used to detect the expression of CCT8 in CRC cells at the transcriptional level (Figure S1A). CRC cell proliferation was assessed by CCK-8 assay. The results showed that reduced CCT8 expression markedly inhibited the proliferation of DLD-1 and HCT116 cells. (Figure S1B, C). Both wound-healing (Figure S1D-F) and Transwell assays (Figure S2) demonstrated that downregulation of CCT8 expression significantly impeded the wound-healing rate and reduced the number of migrating and invading cells. We also demonstrated that reduced CCT8 expression could significantly induce the apoptosis of CRC cells, as indicated by the Annexin V-APC assay (Figure S1G, H). Collectively, CCT8 plays a critical role in CRC progression by promoting cell proliferation, migration, and invasion while inhibiting apoptosis.

CCT8 is correlated with the p53 signaling pathway

We performed GSEA to explore enriched KEGG pathways from CCT8 high-expressed samples. The results contained a total of 40 functional gene sets ($FDR < 0.05$), including pathways such as “cell cycle,” “ubiquitin-mediated proteolysis,” “p53 signaling,” and “ribosome” (Figure S3). The results suggest that CCT8 may promote p53 degradation through ubiquitination with the participation of E3 ligases, among which MDM2 could play a crucial role [12], potentially involving ribosomal pathways.

CCT8 influences the p53 pathway through its coexpressed gene, RPL4

We isolated genes related to CCT8 expression from the TCGA CRC dataset using the R statistical computing language. The results showed that a total of 1392 genes were significantly associated with CCT8. To explore the possible mechanisms of CCT8 in CRC, a PPI network was constructed from the STRING database, and cluster analysis was carried out through the MCODE APP in Cytoscape software. We finally found that the core protein of the CCT8 gene cluster is RPL4 (Fig. 2A).

To further investigate the relationship between CCT8 and RPL4, we analyzed gene transcriptome data downloaded from the UCSC website. Results from the TCGA and GTEx datasets indicated a positive correlation between CCT8 and RPL4 in most tumor tissues (Figure S4A, C), with a similar expression trend in normal tissue (Figure S4B, D). This suggests that CCT8 is coexpressed with RPL4 in both tumor and normal tissues. Validation in CRC and colonic tissues further supported this observation (Figure S4E, F).

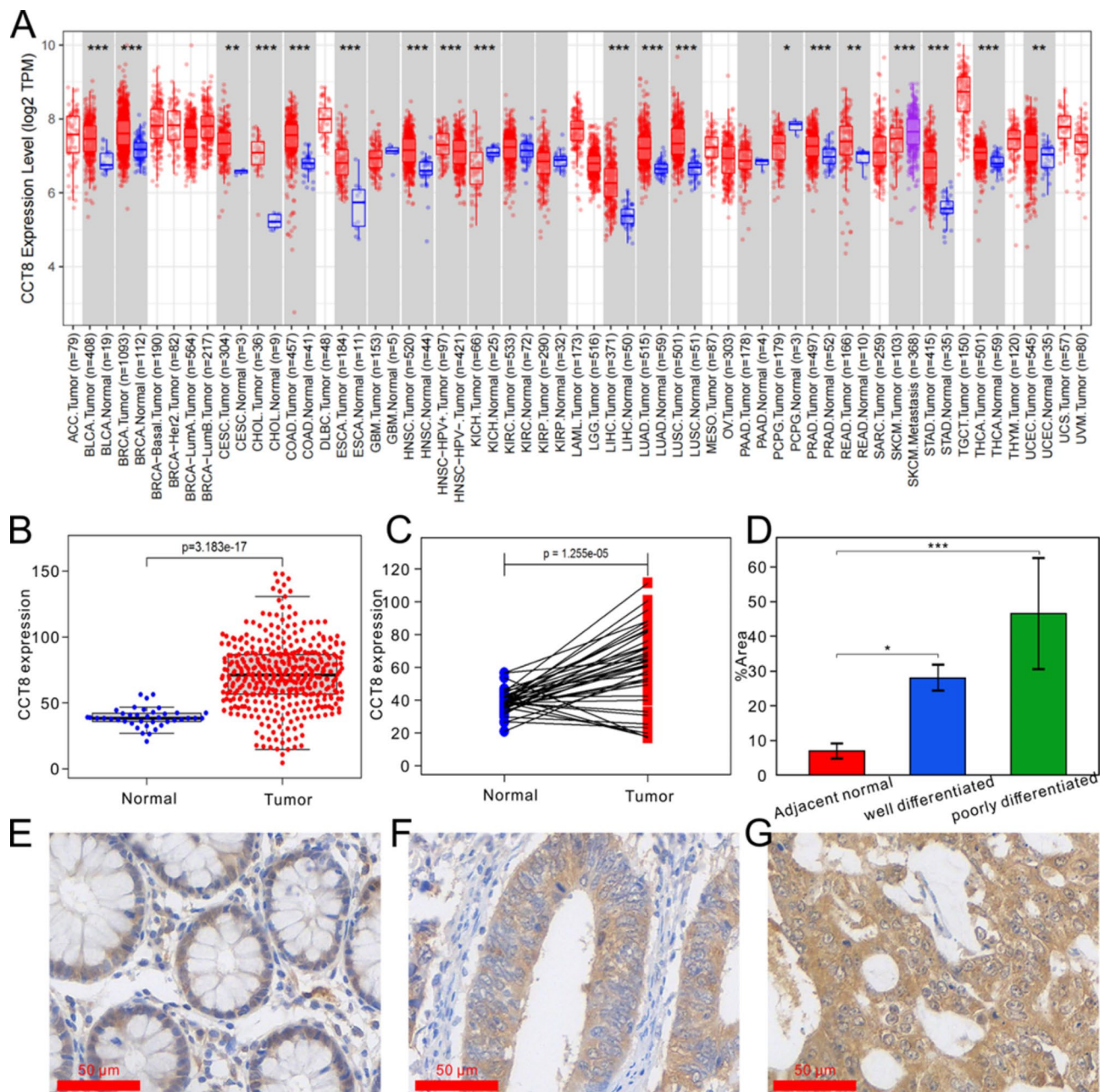


Fig. 1 CCT8 expression. **(A)** The expression of the CCT8 gene in 38 malignant tumors in the TIMER 2.0 database. **(B, C)** The expression level of the CCT8 gene in CRC was significantly higher than that in its paired normal tissues. (Data were analyzed using a Student's t-test) **(D)** The expression rate of the CCT8 gene in poorly differentiated CRC was higher than that in well differentiated CRC. (Data were analyzed using a one-way ANOVA) **(E)** The expression of CCT8 in adjacent normal tissues. **(F)** The expression of CCT8 in well differentiated CRC tissues. **(G)** The expression of CCT8 in poorly differentiated CRC tissues

Immunofluorescence showed the colocalization of CCT8 and RPL4 in the nucleus and cytoplasm (Fig. 2B). As revealed by GST pull-down assay, CCT8 could directly interact with RPL4 (Fig. 2C), which was further confirmed by Co-IP assay (Figs. 2D, E). These results indicate that CCT8 can bind to and interact with RPL4.

CCT8 shows a positive correlation with p53 in most tumor tissues (Figure S4G, I), with a similar expression

trend in normal tissue samples (Figure S4H, J). Interestingly, unlike in normal tissue (Figure S4L), the correlation coefficient between CCT8 and p53 decreases in CRC tissue (Figure S4K). Thus, we consider that CCT8 may mediate the down-regulation of p53 through some mechanisms. In summary, CCT8 may influence the expression of p53 by affecting its coexpressed gene, RPL4.

Table 1 The relationship between CCT8 expression level and clinicopathological features of CRC patients

Clinicopathological features	CCT8 expression level		P value
	Low	High	
Age at diagnosis (years)			0.515 ^a
≥60	27	61	
<60	13	38	
Gender			0.879 ^a
Male	26	63	
Female	14	36	
Tumor location			0.554 ^a
Colon	14	40	
Rectum	26	59	
Tumor size (cm)			0.402 ^a
>5	6	21	
≤5	34	78	
Histological grade			< 0.001 ^a
Low	13	82	
High	27	17	
Metastasis			0.001 ^a
Yes	9	52	
No	31	47	
TMN stage			0.001 ^a
I-II	31	47	
III-IV	9	52	
Mean survival time (months)	48.55	35.48	0.046 ^b

P^a - Chi-Square Test P^b - Kaplan-Meier (log-rank test)

CCT8 promotes the degradation of p53 in the nucleus

To explore the specific relationship between CCT8 and p53, we performed RT-PCR and found that downregulation of CCT8 had no impact on p53 mRNA levels (Fig. 3A). Next, we used actinomycin, a riboprotein reaction inducer, to promote p53 expression and analyzed protein levels via western blotting. These findings indicated a negative correlation between CCT8 and p53 at the protein level (Fig. 3B, D). Then, we found that the downregulation of CCT8 expression extended the half-life of p53 by cycloheximide (CHX) assay (Fig. 3C, E). The inhibitory activity of p53 mainly depends on its nuclear subcellular localization. Thus, immunofluorescence was performed to determine whether the increasing p53 was distributed in the nucleus. The results showed that downregulation of CCT8 increased p53 fluorescence levels, indicating that CCT8 could promote the degradation of p53 in the nucleus (Fig. 3F). Taken together, downregulation of CCT8 expression does not affect p53 mRNA level but upregulates the protein level by prolonging the half-life of p53.

CCT8 enhances the ubiquitylation of p53

Proteasome-mediated degradation is vital in regulating protein homeostasis. To confirm whether the level of p53 was decreased by proteasomal degradation, we treated cells with MG132, a proteasome inhibitor. The results

suggested that downregulation of CCT8 and MG132 could both increase the level of p53 (Fig. 4A). Based on this finding, we speculated that CCT8 could promote the ubiquitin-proteasome system to enhance p53 degradation. To further validate this hypothesis, western blotting and Co-IP assays were used to detect the changes when p53 underwent rapid ubiquitination and proteasome-mediated degradation to determine the effect of CCT8 on total protein ubiquitination and p53 ubiquitination in vivo. Western blotting showed that downregulation of CCT8 hardly affected the total ubiquitin expression level (Fig. 4B), while Co-IP assay demonstrated that the ubiquitination of p53 was significantly inhibited in cells with downregulation of CCT8 (Fig. 4C). E3 ubiquitin ligases are key components in protein ubiquitylation, which determine the specificity of substrates and catalyze the attachment of ubiquitin to substrate proteins. Given that MDM2 is one of the most essential E3 ubiquitin ligases, we conducted western blotting after inhibiting its expression by small interfering RNA to determine the relationship with p53. The results proved that p53 protein was significantly increased following siMDM2 transfection, indicating that the degradation of p53 depended on MDM2 (Fig. 4D). In summary, our findings suggest that CCT8 decreases the level of p53 in CRC by enhancing MDM2-dependent ubiquitylation.

CCT8 influences p53 expression through the RPL4-MDM2-p53 pathway

Previous studies have already established the association between RPLs-MDM2 and p53 [13]. Considering the comprehensive findings, it is plausible that CCT8 may influence p53 expression through the RPL4-MDM2-p53 pathway. We downloaded the gene feature dataset from the GSEA website. GSVA analysis was conducted to score different features for each CRC tumor sample. Subsequently, correlation analysis was performed between the gene expression of CCT8 in corresponding samples. We identified and screened out several crucial pathways potentially associated with CCT8. These include DNA replication, the mechanistic target of rapamycin complex 1 (MTORC1) signaling, MDM2/MDM4 family protein binding, DNA repair, adherens junction, p53 hypoxia pathway, metabolic reprogramming in colon cancer, and Ribosome (Figure S5A-H). Reconfirmed that CCT8 may influence the expression of p53 through the RPL4-MDM2-p53 pathway.

To further determine whether CCT8 breaks the binding with RPL4 and MDM2, we performed Co-IP assays to investigate the interaction with CCT8, RPL4 and MDM2. pCMV-MDM2-Flag, pCMV-RPL4-Myc and pCMV-CCT8-Myc were transfected into HEK293T cells for Co-IP assays (Fig. 5A). The western blot results suggested that RPL4 could interact with MDM2 and that the

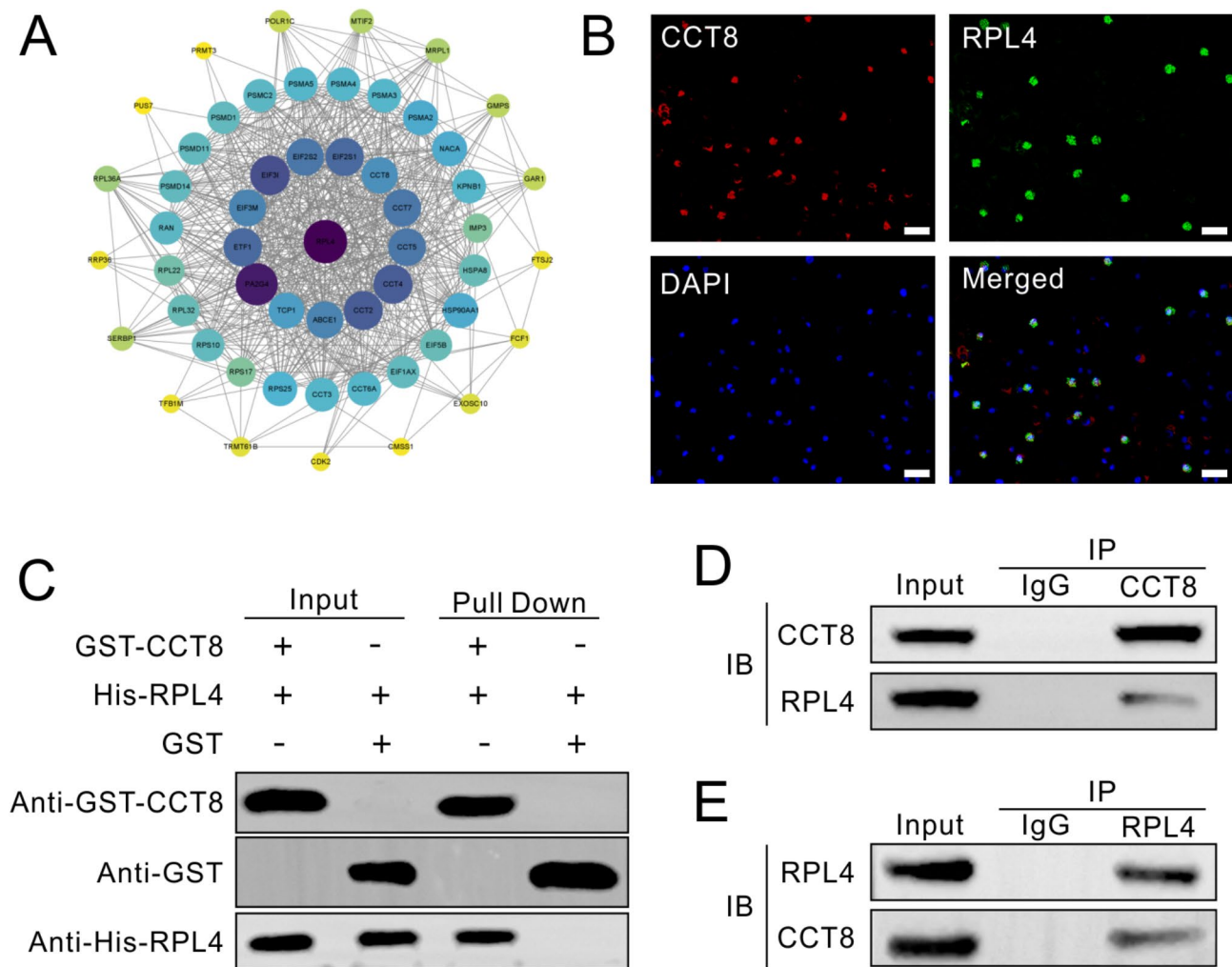


Fig. 2 Relationship between CCT8 and RPL4. **(A)** The PPI network indicated that the core protein of the CCT8 gene cluster is RPL4. **(B)** Immunofluorescence revealed the colocalization of CCT8 and RPL4 in the nucleus and cytoplasm. **(C)** GST pull-down experiments found that RPL4 can interact with CCT8. **(D, E)** Endogenous CCT8 and RPL4 were immunoprecipitated with anti-CCT8 and anti-RPL4 antibodies, and IgG was used as the negative control. The immunocomplexes were analyzed by western blotting. Experiments including gels and blots were repeated three times

binding of MDM2 to RPL4 was reduced after transfection with CCT8, which hinted that CCT8 could disrupt their binding (Fig. 5B). Then, pCMV-p53-Flag, pCMV-Ub-HA, pCMV-RPL4-Myc and pCMV-CCT8-Myc were transfected into HEK293T cells to further verify the mechanism of CCT8 enhancing ubiquitination, and each group was marked with p53-Flag, Ub-HA, RPL4-Myc, CCT8-Myc and GAPDH antibodies. Western blot analysis confirmed that after transfection with RPL4, the ubiquitination of p53 decreased significantly, while CCT8 restored the ubiquitination of p53 (Fig. 5C). The aforementioned results indicate that CCT8 may influence the RPL4-MDM2-p53 pathway by binding with RPL4, thereby facilitating MDM2-mediated ubiquitination of p53.

CCT8 and RPL4 exhibit similar immune infiltration patterns

Previous experiments have confirmed the co-expression of CCT8 and RPL4 in CRC. To further analyze the relationship between them, we conducted an analysis of the immune infiltration patterns of these two genes. Gene sets representing 28 types of immune cells were obtained from the study by Pornpimol Charoentong et al. [14]. Each CRC sample underwent immune infiltration scoring through GSVA analysis and was grouped according to the level of target gene expression. A lower immune infiltration score was observed in the group with increased target gene expression (Figure S5I-J), including activated B cells, eosinophils, natural killer cells, and plasmacytoid dendritic cells. We further analyzed the correlation between CCT8 and RPL4 in terms of gene expression and immune infiltration score, respectively. Significant immune infiltration was noted in CCT8 and

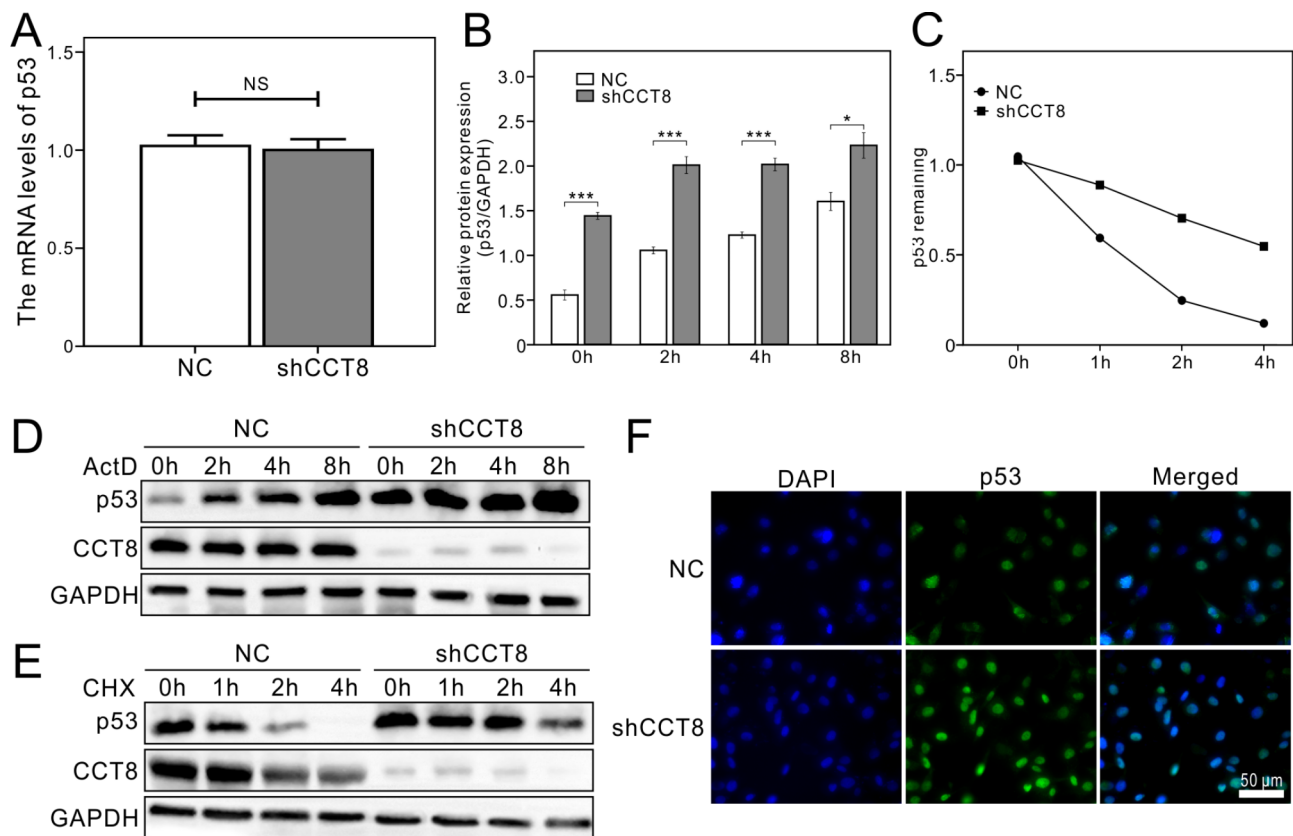


Fig. 3 Negative correlation between CCT8 and p53. **(A)** The mRNA levels of p53 in the shCCT8 group and control group were assessed using RT-PCR. **(B, D)** Western blot analysis revealed that, upon treatment with ActD, the protein level of p53 in the shCCT8 group was significantly higher than that in the NC group. (Data were analyzed using a two-way ANOVA) **(C, E)** When the control group and shCCT8 group were treated with CHX, the half-life of p53 in the shCCT8 group was significantly prolonged compared to that in the NC group. **(F)** Downregulation of CCT8 increased the fluorescence level of p53, and through immunofluorescence, the elevated p53 was identified to localize in the cell nucleus. DAPI was used to visualize the cell nucleus. Experiments including gels and blots were repeated three times

RPL4 genes among activated B cells, eosinophils, natural killer cells, and plasmacytoid dendritic cells. Therefore, we inferred that CCT8 and RPL4 may participate in the same immune mechanism (Figure S5K-L). Additionally, plasmacytoid dendritic cells exhibited the highest correlation coefficient (Figure S5M-N).

Discussion

CCT plays a pivotal role in the folding, unfolding, assembly, and disassembly of new polypeptides, orchestrating the spatial conformation of other proteins [15]. Recent research has underscored a significant correlation between the eight subunits of the CCT protein complex and the advancement of cancer [7, 16, 17]. For instance, CCT3 promotes cell proliferation in thyroid papillary carcinoma and gastric cancer [18, 19], while CCT6 facilitates the onset and progression of liver cancer and non-small cell lung cancer [20, 21]. A groundbreaking study recently published in *CELL* revealed that CCT2 can function as an autophagy receptor, regulating the elimination of protein aggregates and thereby potentially

preventing disease onset [22]. Similarly, CCT8, another key CCT subunit, plays a crucial role in the initiation and progression of a range of tumors [23, 24]. However, the association between CCT8 and cancer remains largely unexplored.

Analysis using Timer 2.0 demonstrated a significantly elevated expression of CCT8 across various digestive tract tumors leading us to focus on CRC for in-depth experimental investigation (Fig. 1A). Immunohistochemical analysis, clinical data and functional assays further underscored the oncogenic potential of CCT8 in CRC. To decipher the underlying mechanisms, we conducted a correlation analysis on CCT8 within data from TCGA datasets. Utilizing the STRING database, we constructed a PPI network, pinpointing core proteins in the CCT8-associated cluster, with RPL4 emerging as a key protein (Fig. 2A). GSEA was performed to pinpoint potential signaling pathways influenced by CCT8, suggesting its involvement in pathways like p53 signaling, ubiquitin-mediated proteolysis and ribosomal functions in CRC (Figure S3).

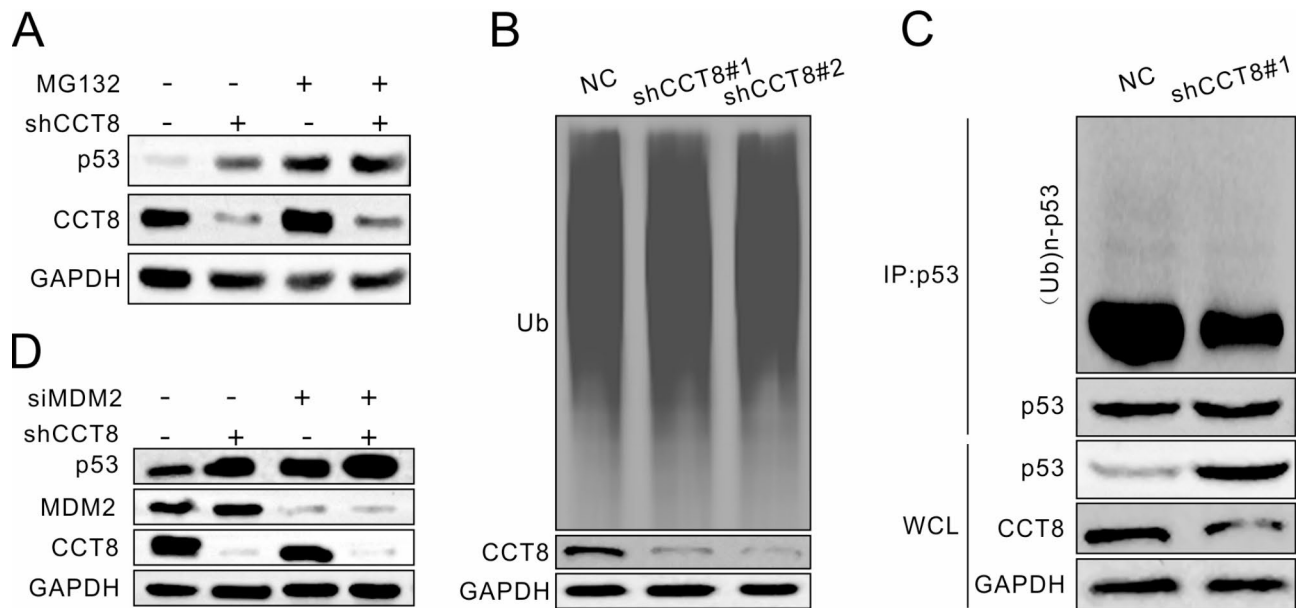


Fig. 4 CCT8 enhances p53 ubiquitylation in CRC. **(A)** The degradation of p53 depends on the activation of the proteasome. Cells in the NC and shCCT8 groups were treated with MG132 (20 μ M) for 6 h. p53 and CCT8 expression was measured by western blotting. **(B)** The differences in Ub, CCT8 and GAPDH protein expression levels were verified by western blotting. **(C)** Whole cell lysates were obtained by cracking cell lines, and the expression levels of GAPDH, CCT8 and p53 were determined by western blotting. **(D)** The expression levels of p53, MDM2, CCT8 and GAPDH were assessed by western blotting. p53 expression was significantly increased in the siMDM2 transfection group. Experiments including gels and blots were repeated three times

To delve deeper into the roles of CCT8 and RPL4 in CRC, we performed an analysis of pan-cancer data using xenata datasets and compared it with normal tissue data from the GTEx datasets. Intriguingly, we found a positive correlation between CCT8 and RPL4 in both cancerous and normal tissues, indicating potential co-expression of these proteins (Figure S4C-D). Additionally, we explored the relationship between CCT8 and p53. Our findings revealed a substantial positive correlation of CCT8 in most normal and pan-cancer tissues (Figure S4G-H). Notably, the correlation coefficient between CCT8 and p53 was reduced in CRC tissues ($0.05 < P < 0.1$) (Figure S4K), but a significant positive correlation persisted in colon tissues (Figure S4L). This led us to hypothesize that CCT8 might play a role in mediating the down-regulation of p53 during the oncogenic transformation of colon tissues.

p53, a pivotal tumor suppressor, is integral in the development and progression of various cancers. While its transcription-independent roles are recognized [25], p53 primarily acts as a transcription factor, initiating the activation of a broad and varied array of target genes. Once activated, p53 orchestrates a wide range of cellular responses [26, 27]. When DNA sustains damage, activated p53 either repairs the cells or induces apoptosis, a process that is critically important for inhibiting the development of nearly all types of cancers [28]. Ubiquitination, a key regulatory pathway of p53, is intimately linked to the degradation of p53 [29]. In healthy cells

under no stress, the levels of p53 are maintained at a low level primarily due to the action of the RING finger E3 ubiquitin ligase, MDM2. The role of MDM2 in ubiquitinating p53 has been established as a contributing factor in the progression of various cancers [30–32]. Initial findings revealed that several RPs bind to MDM2, inhibiting its activity against p53. This interaction leads to the stabilization and activation of p53 [33, 34]. A recent investigation highlighted a specific impairment in p53 signaling in response to ribosomal stress, as opposed to DNA damage [35]. Substantial evidence suggests that RPs play a role in modulating the MDM2-p53 signaling pathway, leading to cellular carcinogenesis, while the relationship between RPL4 and the MDM2-p53 signaling pathway remains unclear. Xia He's study suggested that RPL4 directly interacts with MDM2 at the central acidic domain and suppresses MDM2-mediated p53 ubiquitination and degradation, leading to p53 stabilization and activation [11], and Wuyi Wang's study further proposed that PRDX2 could bind RPL4, reducing the interaction between RPL4 and MDM2 [36]. Yet, the interconnection between CCT8 and the RPL4-MDM2-p53 regulatory loop is still an area that remains unexplored.

To delve deeper into the underlying mechanisms, we began by downloading gene datasets from the GSEA website. Subsequently, each CRC sample was analyzed for distinct characteristics using GSVA. This was followed by a correlation analysis with CCT8 gene expression. We pinpointed and focused on several critical

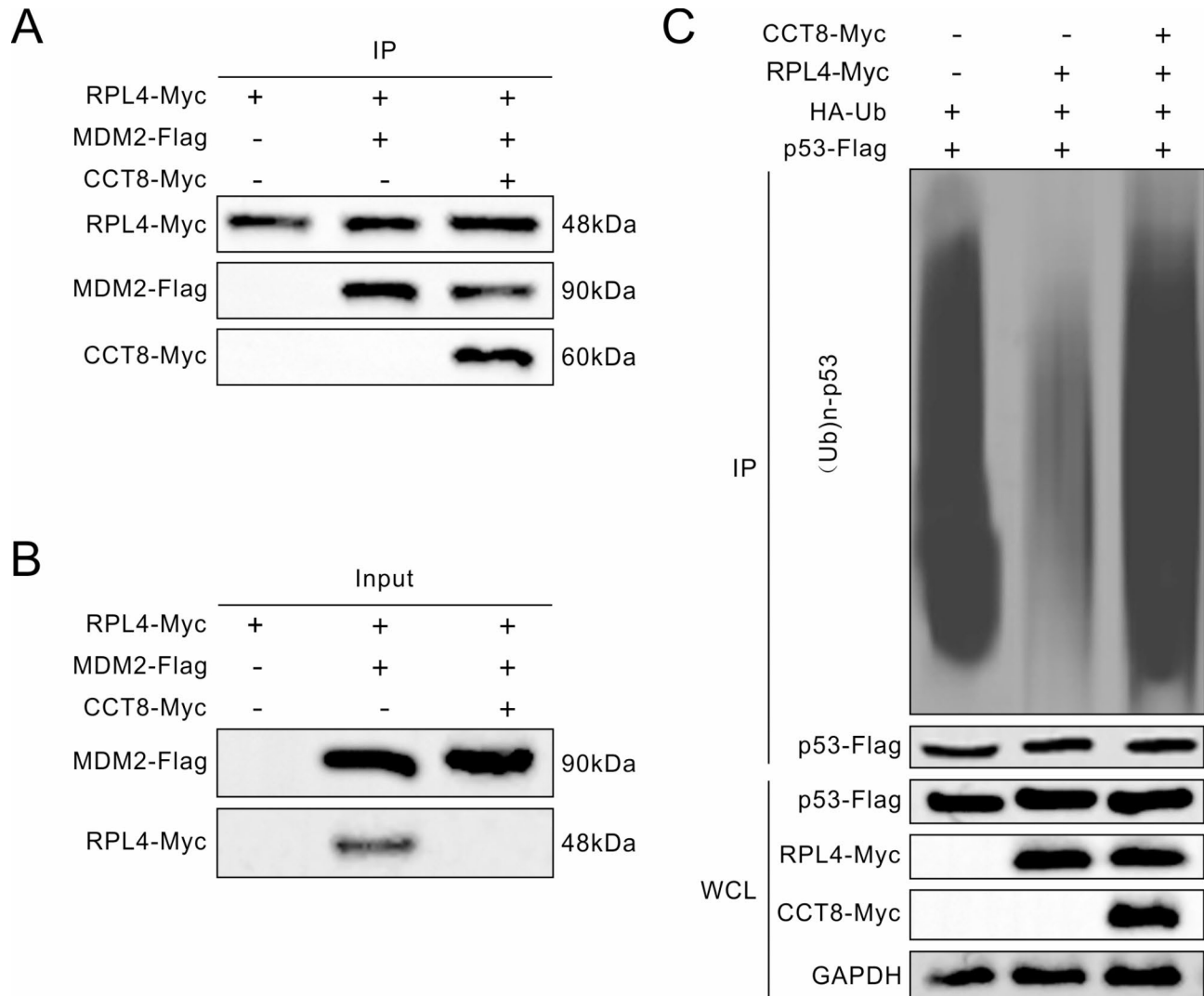


Fig. 5 CCT8 breaks the binding with RPL4 and MDM2. **(A)** HEK293T cells were divided into three groups: Group 1 was transfected with RPL4-Myc, Group 2 was transfected with RPL4-Myc and MDM2-Flag, and Group 3 was transfected with RPL4-Myc, MDM2-Flag and CCT8-Myc. Then, RPL4-Myc, MDM2-Flag and CCT8-Myc antibody markers were used for each group. The transfection efficiency was verified by western blotting. **(B)** MDM2-Flag was pulled down by anti-Flag beads. MDM2-Flag and RPL4-Myc were examined with anti-Myc and anti-Flag antibodies. Western blotting showed reduced binding of MDM2 and RPL4 after transfection with CCT8. **(C)** Group 1 was transfected with p53-Flag and Ub-HA, Group 2 was transfected with p53-Flag, Ub-HA and RPL4-Myc, and Group 3 was transfected with p53-Flag, Ub-HA, RPL4-Myc and CCT8-Myc. Flag-p53 was pulled down by anti-Flag beads and assessed with anti-HA antibodies. Western blotting demonstrated that CCT8 enhances MDM2-mediated p53 proteasomal degradation. Experiments including gels and blots were repeated three times

pathways potentially associated with CCT8, such as DNA replication, MTORC1 signaling, MDM2/MDM4 family protein binding, DNA repair, adherens junctions, the p53 hypoxia pathway, metabolic reprogramming in CRC, and ribosome functioning (Figure S5A-H). Based on these findings, we formulated and substantiated a hypothesis that CCT8 influences the RPL4-MDM2-p53 pathway through its interaction with RPL4, thereby leading to enhanced ubiquitination of p53 by MDM2.

To test our hypothesis, we implemented a series of validating experiments. CHX assays demonstrated an increase in the half-life of the p53 protein following

downregulation of CCT8 (Fig. 3D-E), while MG132 assays confirmed that the proteasome was the critical factor affected by CCT8 in this context (Fig. 4A). Immunoprecipitation experiments revealed an increase in p53 ubiquitination in the nucleus due to CCT8 (Fig. 4B-C). This suggests a strong link between the dysregulation of p53 ubiquitination and CCT8-induced proliferation in CRC. Immunofluorescence experiments indicated that downregulation of CCT8 elevated the fluorescence intensity of p53, which predominantly localized in the nucleus (Fig. 3F). Further analysis using co-immunoprecipitation and western blotting established that CCT8 orchestrates

p53 degradation via ubiquitination in an MDM2-dependent manner (Fig. 4). Additionally, Co-IP and GST pull-down assays confirmed that CCT8 facilitates the ubiquitination and proteasomal degradation of the p53 protein by obstructing the interaction between RPL4 and MDM2 (Fig. 5). These findings lend substantial support to the CCT8-RPL4-MDM2-p53 signaling pathway model (Figure S6).

In recent times, immunotherapy has swiftly become a key treatment approach for various solid tumors, including certain types of CRC. Treatments with immune checkpoint inhibitors, particularly monoclonal antibodies that target programmed cell death 1 and cytotoxic T lymphocyte antigen 4, have shown improved survival rates in metastatic mismatch-repair-deficient or microsatellite instability-high CRC [37]. Various immunotherapeutic agents, such as pembrolizumab, nivolumab, and ipilimumab, have been approved for advanced CRC [38]. The introduction of other immunotherapeutic strategies, including chimeric antigen receptor-modified T cells, monospecific and bispecific antibodies, cellular therapies, vaccines, and cytokines targeting additional immune checkpoints, macrophages, and other elements of innate immunity, has also advanced CRC immunotherapy. Consequently, we sought to investigate the potential significance of the CCT8 and RPL4 relationship in CRC immunotherapy. We analyzed the immune characteristics of CCT8 and RPL4 in CRC using GSVA analysis of expression feature sets from 28 immune cell types. Our findings indicate that overexpression of CCT8 and RPL4 may suppress the expression of activated B cells, eosinophils, natural killer cells, and plasmacytoid dendritic cells, suggesting their involvement in similar immune mechanisms (Figure S5I-J). Notably, plasmacytoid dendritic cells displayed the strongest correlation (Figure S5M-N). Research has demonstrated that the dysfunction of plasmacytoid dendritic cells is closely linked with the advancement of various tumors and is a focus of cancer immunotherapy [39]. These insights underscore the considerable potential of our study in validating the co-expression of CCT8 and RPL4 as a potential biomarker in CRC immunotherapy.

However, certain limitations remain. The limited sample size in immunohistochemical analysis may affect the statistical reliability of survival analysis, and there is a lack of direct *in vivo* evidence such as animal models. In future research, we aim to expand the immunohistochemical sample size, establish xenograft mouse models, and further investigate the molecular regulatory mechanisms of CCT8 in CRC. These efforts will provide more robust experimental evidence to validate and extend our key findings, ultimately contributing to precision oncology.

Conclusion

Our study reveals the oncogenic role of CCT8 in CRC and its mechanism of regulating tumor cell behavior through the RPL4-MDM2-p53 axis (Figure S6). Targeting the CCT8-RPL4 interaction could pave new paths for improving survival rates in CRC patients and developing innovative cancer treatments. Our research provides crucial insights into the molecular mechanisms of CRC and the development of therapeutic strategies.

Abbreviations

CCT	Chaperonin Containing TCP1 Complex
CCK-8	Cell Counting Kit 8
CHX	Cycloheximide
Co-IP	Co-immunoprecipitation
CRC	Colorectal Cancer
FDR	False Discovery Rate
GEO	Gene Expression Omnibus
GSEA	Gene Set Enrichment Analysis
GST	Glutathione-S-Transferase
GTex	Genotype-Tissue Expression
GSVA	Gene Set Variation Analysis
KEGG	Kyoto Encyclopedia of Genes and Genomes
MDM2	Murine double minute 2
PPI	Protein-Protein Interaction
RP	Ribosomal Protein
TCGA	The Cancer Genome Atlas

Supplementary Information

The online version contains supplementary material available at <https://doi.org/10.1186/s12920-025-02133-4>.

Supplementary Material 1
 Supplementary Material 2
 Supplementary Material 3
 Supplementary Material 4
 Supplementary Material 5
 Supplementary Material 6
 Supplementary Material 7
 Supplementary Material 8
 Supplementary Material 9
 Supplementary Material 10
 Supplementary Material 11
 Supplementary Material 12
 Supplementary Material 13

Acknowledgements

The authors would like to thank all participants who contributed to the study.

Author contributions

Conceptualization, X.X. and Z.C.; Methodology, Y.T.; Validation, Y.T., Z.L., H.L. and X.L.; Formal analysis, Z.L.; Investigation, X.L.; Resources, H.L.; Data curation, B.P., Y.Z., Q.Y., J.G., Y.R. and D.L.; Writing—original draft preparation, H.L.; Writing—review and editing, Y.T.; Visualization, X.L. and Z.L.; Supervision, X.X. and Z.C.; Project administration, X.X. and Z.C.; Funding acquisition, X.X. and Z.C. All authors have read and agreed to the published version of the manuscript.

Funding

This research was supported by the 2023 Medical and Health Science and Technology Plan of Zhejiang Province (Project No. 2023KY908).

Data availability

No datasets were generated or analysed during the current study.

Declarations**Ethics approval**

Not applicable.

Consent to participate

Not applicable.

Consent to publish

Not applicable.

Competing interests

The authors declare no competing interests.

Received: 14 December 2024 / Accepted: 26 March 2025

Published online: 18 April 2025

References

- Fitzmaurice C, Akinyemiju TF, Al Lami FH, et al. Global, regional, and National cancer incidence, mortality, years of life lost, years lived with disability, and Disability-Adjusted life-Years for 29 cancer groups, 1990 to 2016: A systematic analysis for the global burden of disease study. *JAMA Oncol.* 2018;1(11):1553–68. <https://doi.org/10.1001/jamaoncol.2018.2706>.
- Bray F, Ferlay J, Soerjomataram I, Siegel RL, Torre LA, Jemal A. Global cancer statistics 2018: GLOBOCAN estimates of incidence and mortality worldwide for 36 cancers in 185 countries. *CA: cancer J Clin.* 2018;68(6):394–424. <https://doi.org/10.3322/caac.21492>.
- Buskermolen M, Cenin DR, Helsing LM, et al. Colorectal cancer screening with faecal immunochemical testing, sigmoidoscopy or colonoscopy: a microsimulation modelling study. *BMJ (Clinical Res ed).* 2019;367:15383. <https://doi.org/10.1136/bmj.15383>.
- Testa U, Pelosi E, Castelli G. Colorectal cancer: genetic abnormalities, tumor progression, tumor heterogeneity, clonal evolution and tumor-initiating cells. *Medical sciences (Basel, Switzerland).* 2018;13(2). <https://doi.org/10.3390/medsci6020031>.
- Grantham J. The molecular chaperone CCT/TRiC: an essential component of proteostasis and a potential modulator of protein aggregation. *Front Genet.* 2020;11:172. <https://doi.org/10.3389/fgene.2020.00172>.
- Llorca O, Martín-Benito J, Grantham J, et al. The 'sequential allosteric ring' mechanism in the eukaryotic chaperonin-assisted folding of actin and tubulin. *EMBO J.* 2001;1(15):4065–75. <https://doi.org/10.1093/emboj/20.15.4065>.
- Liao Q, Ren Y, Yang Y, et al. CCT8 recovers WTP53-suppressed cell cycle evolution and EMT to promote colorectal cancer progression. *Oncog.* 2021;3(12):84. <https://doi.org/10.1038/s41389-021-00374-3>.
- Lane D, Levine A. p53 research: the past Thirty years and the next Thirty years. *Cold Spring Harbor Perspect Biology.* 2010;2(12):a000893. <https://doi.org/10.1101/cshperspect.a000893>.
- Joerger AC, Fersht AR. The p53 pathway: origins, inactivation in cancer, and emerging therapeutic approaches. *Annual Rev Biochem.* 2016;85:375–404. <https://doi.org/10.1146/annurev-biochem-060815-014710>.
- Michael D, Oren M. The p53-Mdm2 module and the ubiquitin system. *Semin Cancer Biol.* 2003;13(1):49–58. [https://doi.org/10.1016/s1044-579x\(02\)00099-8](https://doi.org/10.1016/s1044-579x(02)00099-8).
- He X, Li Y, Dai MS, Sun XX. Ribosomal protein L4 is a novel regulator of the MDM2-p53 loop. *Oncotarget.* 2016;29(13):16217–26. <https://doi.org/10.18632/oncotarget.7479>.
- Möll UM, Petrenko O. The MDM2-p53 interaction. *Mol Cancer Res.* 2003;1(14):1001–8.
- Liu Y, Deisenroth C, Zhang Y. RP-MDM2-p53 pathway: linking ribosomal biogenesis and tumor surveillance. *Trends Cancer.* 2016;2(4):191–204. <https://doi.org/10.1016/j.trecan.2016.03.002>.
- Charoentong P, Finotello F, Angelova M et al. Pan-cancer Immunogenomic Analyses Reveal Genotype-Immunophenotype Relationships and Predictors of Response to Checkpoint Blockade. *Cell Rep.* 2017;18(1):248–262. <https://doi.org/10.1016/j.celrep.2016.12.019>
- Huang X, Wang X, Cheng C, et al. Chaperonin containing TCP1, subunit 8 (CCT8) is upregulated in hepatocellular carcinoma and promotes HCC proliferation. *Apmis.* 2014;122(11):1070–9. <https://doi.org/10.1111/apm.12258>.
- Xu WX, Song W, Jiang MP, et al. Systematic characterization of expression profiles and prognostic values of the eight subunits of the chaperonin tric in breast cancer. *Front Genet.* 2021;12:637887. <https://doi.org/10.3389/fgene.2021.637887>.
- Qiu X, He X, Huang Q et al. Oct. Overexpression of CCT8 and its significance for tumor cell proliferation, migration and invasion in glioma. *Pathology, research and practice.* 2015;211(10):717–25. <https://doi.org/10.1016/j.prp.2015.04.012>
- Shi X, Cheng S, Wang W. Suppression of CCT3 inhibits malignant proliferation of human papillary thyroid carcinoma cell. *Oncol Lett.* 2018;15(6):9202–8. <https://doi.org/10.3892/ol.2018.8496>.
- Birbo B, Madu EE, Madu CO, Jain A, Lu Y. Role of HSP90 in cancer. *Int J Mol Sci.* 2021;25(19). <https://doi.org/10.3390/ijms221910317>.
- Ying Z, Tian H, Li Y, et al. CCT6A suppresses SMAD2 and promotes prometastatic TGF- β signaling. *J Clin Invest.* 2017;1(5):1725–40. <https://doi.org/10.1172/jci90439>.
- Zeng G, Wang J, Huang Y, et al. Overexpressing CCT6A contributes to cancer cell growth by affecting the G1-To-S phase transition and predicts A negative prognosis in hepatocellular carcinoma. *OncoTargets Therapy.* 2019;12:10427–39. <https://doi.org/10.2147/ott.s229231>.
- Ma X, Lu C, Chen Y et al. CCT2 is an aggrephagy receptor for clearance of solid protein aggregates. *Cell.* 2022;185(8):1325–1345.e22. <https://doi.org/10.1016/j.cell.2022.03.005>
- Liu P, Kong L, Jin H, Wu Y, Tan X, Song B. Differential secretome of pancreatic cancer cells in serum-containing conditioned medium reveals CCT8 as a new biomarker of pancreatic cancer invasion and metastasis. *Cancer Cell Int.* 2019;19:262. <https://doi.org/10.1186/s12935-019-0980-1>.
- Yin H, Miao X, Wu Y, et al. The role of the chaperonin containing t-complex polypeptide 1, subunit 8 (CCT8) in B-cell non-Hodgkin's lymphoma. *Leuk Res.* 2016;45:59–67. <https://doi.org/10.1016/j.leukres.2016.04.010>.
- Ho T, Tan BX, Lane D. How the other half lives: what p53 does when it is not being a transcription factor. *Int J Mol Sci.* 2019;18(1). <https://doi.org/10.3390/ijms21010013>.
- Murray-Zmijewski F, Slee EA, Lu X. A complex barcode underlies the heterogeneous response of p53 to stress. *Nat Reviews Mol Cell Biology.* 2008;9(9):702–12. <https://doi.org/10.1038/nrm2451>.
- Jiang L, Kon N, Li T, et al. Ferroptosis as a p53-mediated activity during tumour suppression. *Nat.* 2015;520(7545):57–62. <https://doi.org/10.1038/nature14344>.
- Huang Y, Jiao Z, Fu Y, et al. An overview of the functions of p53 and drugs acting either on wild- or mutant-type p53. *Eur J Med Chem.* 2024;3:265:116121. <https://doi.org/10.1016/j.ejmech.2024.116121>.
- Chao CC. Mechanisms of p53 degradation. *Clin Chim Acta.* 2015;1:438:139–47. <https://doi.org/10.1016/j.cca.2014.08.015>.
- Haupt S, Vijayakumaran R, Miranda PJ, Burgess A, Lim E, Haupt Y. The role of MDM2 and MDM4 in breast cancer development and prevention. *J Mol Cell Biol.* 2017;1(1):53–61. <https://doi.org/10.1093/jmcb/mjx007>.
- Dey DK, Sharma C, Vadlamudi Y, Kang SC. CopA3 peptide inhibits MDM2-p53 complex stability in colorectal cancers and activates p53 mediated cell death machinery. *Life Sci.* 2023;318:121476. <https://doi.org/10.1016/j.lfs.2023.121476>.
- Meng X, Franklin DA, Dong J, Zhang Y. MDM2-p53 pathway in hepatocellular carcinoma. *Cancer Res.* 2014;15(24):7161–7. <https://doi.org/10.1158/0008-5472.Can-14-1446>.
- Dai MS, Lu H. Inhibition of MDM2-mediated p53 ubiquitination and degradation by ribosomal protein L5. *J Biol Chem.* 2004;22(43):44475–82. <https://doi.org/10.1074/jbc.M403722200>.
- Zhang Y, Wolf GW, Bhat K, et al. Ribosomal protein L11 negatively regulates oncoprotein MDM2 and mediates a p53-dependent ribosomal-stress checkpoint pathway. *Mol Cell Biology.* 2003;23(23):8902–12. <https://doi.org/10.1128/mcb.23.23.8902-8912.2003>.
- Macias E, Jin A, Deisenroth C, et al. An ARF-independent c-MYC-activated tumor suppression pathway mediated by ribosomal protein-Mdm2 interaction. *Cancer Cell.* 2010;14(3):231–43. <https://doi.org/10.1016/j.ccr.2010.08.007>.

36. Wang W, Wei J, Zhang H, et al. PRDX2 promotes the proliferation of colorectal cancer cells by increasing the ubiquitinated degradation of p53. *Cell Death Dis.* 2021;11(6):605. <https://doi.org/10.1038/s41419-021-03888-1>.
37. Ganesh K, Stadler ZK, Cercek A, et al. Immunotherapy in colorectal cancer: rationale, challenges and potential. *Nat Rev Gastroenterol Hepatol.* 2019;16(6):361–75. <https://doi.org/10.1038/s41575-019-0126-x>.
38. Zhao W, Jin L, Chen P, Li D, Gao W, Dong G. Colorectal cancer immunotherapy-Recent progress and future directions. *Cancer Lett.* 2022;1:545:215816. <https://doi.org/10.1016/j.canlet.2022.215816>.
39. Fu C, Zhou L, Mi QS, Jiang A. Plasmacytoid dendritic cells and cancer immunotherapy. *Cells.* 2022;11(2). <https://doi.org/10.3390/cells11020222>.

Publisher's note

Springer Nature remains neutral with regard to jurisdictional claims in published maps and institutional affiliations.